

# High Energy $\gamma$ -ray variability of NGC 1275 and 3C 120

Narek Sahakyan

ICRANet-Armenia, Marshall Baghramian Avenue 24a, Yerevan 0019, Armenia  
email: [narek@icra.it](mailto:narek@icra.it)

**Abstract.** The recent observations in the high energy  $\gamma$ -ray band show that the extragalactic  $\gamma$ -ray sky is dominated by the emission from blazars. However,  $\gamma$ -ray emission from other types of AGNs, e.g., radiogalaxies, also have been detected. These sources were not considered as favored GeV emitters because the nonthermal emission from their jets is less Doppler boosted. Now, the  $\gamma$ -ray emission from more than 25 non-blazar AGNs has been already detected which opened a new window to have an insight into the particle acceleration and emission processes in different components of AGNs. Here, I will present the  $\gamma$ -ray variability of two well-known radiogalaxies, NGC 1275 and 3C 120, which show a rapid flux increase in the  $\gamma$ -ray band.

**Keywords.** galaxies: active, galaxies: individual (NGC 1275, 3C 120), gamma rays: observations

---

## 1. Introduction

The recent observations in the High Energy (HE;  $\geq 100$  MeV)  $\gamma$ -ray band show that the extragalactic  $\gamma$ -ray sky is dominated by the emission of Active Galactic Nuclei (AGNs) of different types (Acero *et al.* (2015)). Dominant in these are blazars - an extreme class of AGNs which have jets that are forming a small angle with respect to the line of sight (Urry & Padovani (1995)). Blazars are very bright and luminous sources known to emit electromagnetic radiation in almost all frequencies that are currently being observed, ranging from radio to very high energy  $\gamma$ -ray bands. Their broadband spectrum is mainly dominated by non-thermal emission produced in a relativistic jet pointing toward the observer. Other important class of  $\gamma$ -ray emitting AGNs observed by Fermi Large Area Telescopes (Fermi LAT) are radio galaxies with relativistic jets at systematically larger angles (Sahakyan *et al.* (2018)). Due to larger jet inclination angle as compared with blazars, the jet emission is not significantly Doppler boosted, making it less prevalent over such components as the radiation from mildly relativistic outflows or emission from extended structures. This providing a chance to investigate also the emission from extended non-boosted regions, moderately relativistic plasmas, etc.

Only a very small fraction of the total AGNs detected by Fermi-LAT (2%) are non-blazar AGNs, including fourteen radio galaxies, six SSRQs, one CSSs and five NLSy1s. The radio galaxies detected in the  $\gamma$ -ray band can be sub-divided into two morphological types, FRI and FRII (Fanaroff & Riley (1974)), according to their radio luminosities. FRIs have a typical luminosity of  $< 10^{41}$  erg s $^{-1}$  (at 178 MHz) while that of the luminous FRIIs is  $> 10^{41}$  erg s $^{-1}$  (at 178 MHz). FRIs have slower, more turbulent and less collimated jets, while FRIIs have powerful collimated jets (often only one is visible) which terminate into well-defined lobes with prominent hot spots. Increasingly aligned versions of FRIIs are SSRQs, which are powerful radio sources with large-scale radio structures and which appear at intermediate angles between FRIIs and FSRQs. SSRQs are sometimes classified as CSS quasars, since most of the radio flux is emitted within galactic scales ( $< 10$  kpc) rather than at hundreds of kilo-parsec scales.

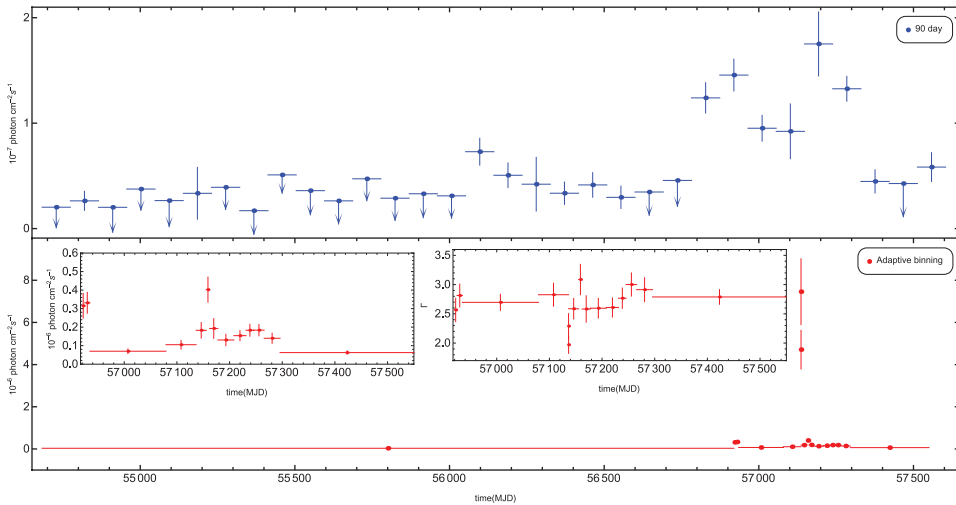


**Figure 1.** The  $\gamma$ -ray light curve of 3C 120 from August 4, 2008, to August 4, 2016 with 90 days bin (a) and 20 % of uncertainty (b).

The recent studies showed that the  $\gamma$ -ray photon index of non-blazar AGNs changes within 1.84 – 2.86 (Sahakyan *et al.* (2018)). The hardest photon indexes of  $\Gamma = 1.84 \pm 0.17$  and  $\Gamma = 1.89 \pm 0.04$  were obtained for TXS 0331+3915 and PKS 0625-35, respectively. The measured faintest flux is of the order of a few times  $10^{-9}$  photon  $\text{cm}^{-2}\text{s}^{-1}$ , while the flux from bright sources exceeds  $10^{-7}$  photon  $\text{cm}^{-2}\text{s}^{-1}$ . In the  $\Gamma - F_{\gamma}$  plane, the FRIs have a harder  $\gamma$ -ray photon index with  $\Gamma_m \simeq 2.22$  and a flux ranging from  $\simeq 1.5 \times 10^{-9} \times \text{photon cm}^{-2}\text{s}^{-1}$  to  $3.6 \times 10^{-8} \times \text{photon cm}^{-2}\text{s}^{-1}$ . The mean photon index of FRIs/SSRQs shifts to a higher value of  $\Gamma_m \simeq 2.58$  (i.e., softer spectra) and the flux to the range of  $(0.9 - 4) \times 10^{-8}$  photon  $\text{cm}^{-2}\text{s}^{-1}$ .

The  $\gamma$ -ray emission from most of the non-blazars AGNs is variable in a long-timescales and only for NGC 1275 and 3C 120 extreme short time scale variabilities are found. Here, I briefly review the main results of the  $\gamma$ -ray observations of NGC 1275 (Baghmanyan *et al.* (2017)) and 3C 120 (Sahakyan *et al.* (2015), Zargaryan *et al.* (2017)), mainly discussing the temporal variation of the  $\gamma$ -ray flux.

## 2. 3C 120

At the red shift  $z = 0.033$ , 3C 120 is a nearby Seyfert 1 radio galaxy that is an active and powerful emitter of radiation at all the observed wavebands. With bright continuum and broad optical emission lines 3C 120 is usually classified as a broad line radio galaxy. Hosting a black hole with a mass  $5.5 \times 10^7 M_{\odot}$  (Peterson *et al.* (2004)), well constrained from the reverberation mapping, 3C 120 has a radio morphology more similar to the FR I radio sources. The source has a powerful one-sided radio jet extending from a sub- $pc$  up to 100  $kpc$  scales (Walker *et al.* (1987)). Observations with the Very Long Baseline Array at frequencies (22, 43, and 86 GHz) reveal a very rich inner jet structure containing several superluminal components with apparent speed up to 4-6  $c$  (e.g., Homan *et al.* (2001)) that can be investigated with better resolution than most other extragalactic superluminal sources because of the relatively low redshift. The jet inclination angle to the line of sight is constrained to be  $14^{\circ}$  by the measured apparent motion. Recently, using X-ray and radio observations, Marscher *et al.* (2002) found that dips in the X-ray emission are followed by ejections of bright superluminal knots in the radio jet, which clearly establishes an accretion-disk-jet connection.

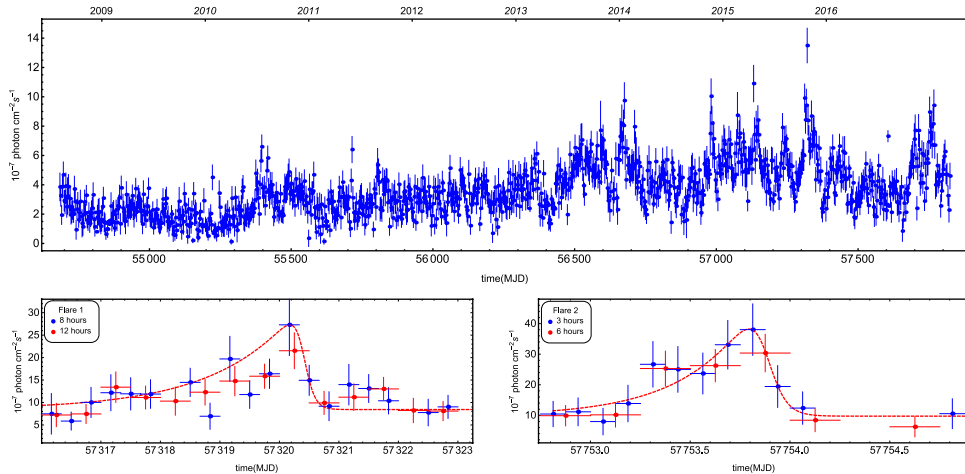


**Figure 2.** The  $\gamma$ -ray light curve of NGC 1275 from August 4, 2008 to March 5, 2017, with 3-day (blue) binning. *Lower panels:* Sub intervals covering F1 (left) and F2 (right).

The  $\gamma$ -ray light curve of 3C 120 from August 4, 2008, to August 4, 2016 obtained for 90-day binning is shown in the upper panel of Fig. 1 (from Zargaryan *et al.* (2017)). Before  $\approx$  MJD 56000 (March 14, 2012), the source is mostly undetectable by Fermi LAT. Then the source flux was high enough to be detected by Fermi LAT, and up to  $\approx$  MJD 56800 it remained constant with no significant changes. Starting from  $\approx$  MJD 56800, the flux substantially increased up to a few times  $10^{-7}$  photon  $\text{cm}^{-2} \text{s}^{-1}$  and remained so till  $\approx$  MJD 57350. The same light curve 20% adaptively binned intervals is shown in lower panel in Fig. 1. As it is expected, initially it took a long time to reach the necessary 20 % uncertainty. Indeed, the first bin contains the data from the start of the mission to MJD 56919.31 (19 September 2014), amounting to more than 6 years. Afterwards, it took shorter time to reach the required uncertainty. The most dramatic increase in the  $\gamma$ -ray flux was observed on April 24, 2015. First, within 19.0 min the flux reached  $(7.46 \pm 1.56) \times 10^{-6}$  photon  $\text{cm}^{-2} \text{s}^{-1}$  with  $\Gamma = 2.29 \pm 0.21$  and  $11.2\sigma$  detection significance. Then for another 3.15 hours it was as high as  $(4.71 \pm 0.92) \times 10^{-6}$  photon  $\text{cm}^{-2} \text{s}^{-1}$  with  $\Gamma = 1.97 \pm 0.14$  and  $12.7\sigma$ . Then the flux slowly decreased down to a few times  $10^{-7}$  photon  $\text{cm}^{-2} \text{s}^{-1}$  with the bin size varying within 10 to 35 days. The source was in an active state up to  $\approx$  MJD 57300 and then turned again into its quiescent state, in which case the data should be accumulated for  $\approx 254$  days.

### 3. NGC 1275

Due to its proximity ( $z = 0.0176$ ,  $\approx 75.6$  Mpc) and brightness, the radio galaxy NGC 1275 has been a target for observations in almost all energy bands. Core-dominated asymmetrical jets at both kpc (Pedlar *et al.* (1990)) and pc (Asada *et al.* (2006)) scales have been detected in the radio band with characteristics more similar to those of FR1 sources. The emission in the X-ray band is mostly dominated by the thermal emission from the cluster, although a nonthermal component in the energy range 0.5-10 keV with a photon index of  $\Gamma_X = 1.65$  has been observed (Churazov *et al.* (2003)).

Fig. 2 (upper panel) shows the  $\gamma$ -ray light curve with three-day bin size. Despite the fact that the flux sometimes exceeded the averaged value presented in 3FGL ( $\approx 2.26 \times 10^{-7}$  photons  $\text{cm}^{-2} \text{s}^{-1}$ ), pronounced flaring activities were detected in October 2015 (hereafter Flare 1 [F1]) and in December 2016/January 2017 (hereafter Flare 2 [F2]). Starting from 22 October 2015 the daily averaged flux of NGC 1275 was above

$10^{-6}$  photons  $\text{cm}^{-2} \text{s}^{-1}$  and remained high for 5 days with a daily averaged maximum of  $(1.48 \pm 0.20) \times 10^{-6}$  photons  $\text{cm}^{-2} \text{s}^{-1}$  observed on 24 October 2015. Another substantial increase in the  $\gamma$ -ray flux was observed on December 31, 2016 when the flux increased from about  $(4 \sim 5) \times 10^{-7}$  photons  $\text{cm}^{-2} \text{s}^{-1}$  to  $(2.21 \pm 0.26) \times 10^{-6}$  photons  $\text{cm}^{-2} \text{s}^{-1}$  within a day with a detection significance of  $\sim 21.5\sigma$ .

During F1 and F2, the flare time profiles are investigated by fitting them with double exponential functions (Abdo *et al.* (2010)). The corresponding fit is shown in Fig. 2 lower panels (from Baghmanyan *et al.* (2017)). The time profiles show asymmetric structures in both flares, showing a slow rise and a fast decay trend. The time peak of the flares calculated by  $t_p = t_0 + t_r t_d / (t_r + t_d) \ln(t_d / t_r)$  is MJD 57320.18 for F1 with the maximum intensity of  $(2.39 \pm 0.31) \times 10^{-6}$  photon  $\text{cm}^{-2} \text{s}^{-1}$ . The rise time is  $32.49 \pm 7.20$  hours with a sudden drop within  $2.22 \pm 1.19$  hours. The parameters of F2 are better estimated and are characterized with a shorter rise time, when within  $8.03 \pm 1.24$  hours the flux reaches its maximum of  $(4.20 \pm 0.48) \times 10^{-6}$  photon  $\text{cm}^{-2} \text{s}^{-1}$  on MJD 57753.79 and drops nearly 4 times in  $\sim 6$  hours. The minimal e-folding time is  $t_d = 1.21 \pm 0.22$  hours, using the decay time scale of F2, and it is the most rapid  $\gamma$ -ray variability observed for NGC 1275. We note that even if the rise time of F2 is used, the flux e-folding time of about  $8.03 \pm 1.24$  hours will still be shorter than any previously reported value.

## References

- Abdo, A. A., Ackermann, M., Ajello, M., *et al.* 2010, *ApJ*, 722, 520  
Acero, F., Ackermann, M., Ajello, M., *et al.* 2015, *ApJ*, 218, 23  
Asada, K., Kamenno, S., Shen, Z.-Q., *et al.* 2006, *PASJ*, 58, 261  
Baghmanyan, V., Gasparyan, S., & Sahakyan, N. 2017, *ApJ*, 848, 111  
Churazov, E., Forman, W., Jones, C., & Böhringer, H. 2003, *ApJ*, 590, 225  
Fanaroff, B. L., & Riley, J. M. 1974, *MNRAS*, 167, 31P  
Homan, D. C., Ojha, R., Wardle, J. F. C., *et al.* 2001, *ApJ*, 549, 840  
Marscher, A. P., Jorstad, S. G., Gómez, J.-L., *et al.* 2002, *Nature*, 417, 625  
Pedlar, A., Ghataure, H. S., Davies, R. D., *et al.* 1990, *MNRAS*, 246, 477  
Peterson, B. M., Ferrarese, L., Gilbert, K. M., *et al.* 2004, *ApJ*, 613, 682  
Sahakyan, N., Zargaryan, D., & Baghmanyan, V. 2015, *A&A*, 574, A88  
Sahakyan, N., Baghmanyan, V., & Zargaryan, D. 2018, *A&A*, 614, A6  
Urry, C. M., & Padovani, P. 1995, *PASP*, 107, 803  
Walker, R. C., Benson, J. M., & Unwin, S. C. 1987, *ApJ*, 316, 546  
Zargaryan, D., Gasparyan, S., Baghmanyan, V., & Sahakyan, N. 2017, *A&A*, 608, A37